Power Factor control for High efficiency operation of An Open-Ended Winding motor Using A Dual inverter Drive With A Floating Bridge

C.K Babu[1], S. Venkat Rao[2]
[2] associate professor
[1, 2] SRI VENKATESA PERUMAL COLLEGE OF ENGINEERING AND TECHNOLOGY

Abstract- *A novel control scheme is presented for an open-ended winding motor dual inverter drive, where a primary inverter is supplied from a dc power source and a secondary inverter is supplied from a floating dc capacitor with no power source. Examination of the basic single phase equivalent circuit model of an induction machine reveals that near optimal motor efficiency is achieved at a relatively constant motor fundamental power factor over a wide range of motor loads and drive operating frequencies, e.g. 0.71 for the motor used in this work. The drive control described uses the phase difference between the fundamental output voltages of the primary and secondary converters in order to control the motor's terminal voltage and to maintain a motor power factor of 0.71. This control is maintained over the full range of the motor's load and drive frequency settings. The floating capacitor bridge voltage is regulated using PI feedback control, with the capacitor voltage error signal as the input and the amplitude modulation index of the primary inverter as the output. The capacitor voltage reference signal is related to the per-unit drive frequency and measured current: as the motor's current or frequency changes, the capacitor's voltage reference is updated in a proportional manner to both parameters. This control approach keeps the fundamental phase difference between the two inverters within a stable operating range, maintains the power factor of the main bridge close to unity, and improves the floating bridge's dc capacitor voltage stability during transient load changes. The drive control performance is presented using detailed simulations and experimental testing; verifying the regulation of the floating capacitor's voltage as well as the predicted efficiency gains for the induction motor under constant power factor operation as compared with conventional drive control.*

Keywords- variable frequency drive; power factor control; open end winding induction machine (OEWIM); dual inverter drive (DID); floating bridge

I. INTRODUCTION

Over the last decade the open-ended induction motor and dual inverter drive (DID) topology has gained attention as a practical high efficiency variable frequency motor drive system. The primary benefits of this drive include: boosting of the motor's terminal voltage; an improved pulse-width modulation (PWM) motor supply voltage (increased PWM frequency using multilevel waveforms); and improved motor performance in the speed extension region . In addition, the duality of the DID topology makes it more reliable than other multilevel converter topologies, as a failure in one converter still allows for motor operation from the complementary three-phase inverter. The multilevel nature and voltage boosting capability of the DID make it ideal for medium voltage and high power applications, or low voltage applications demanding high frequencies.

Multiple three-level PWM strategies have been developed for DIDs supplied by two isolated dc sources. However, in practical applications a bulky phase-shifting isolating transformer is required to maintain the secondary isolated dc source. Therefore, the most common approach is to supply both the primary and secondary converters with a single common dc source, thus eliminating the requirement of the additional transformer. This topology creates pathways for zero-sequence common-mode currents to circulate within the system, which can distort the motor's supply current and increase conduction losses . These currents may be suppressed through the use of bulky common-mode choke inductors, or an additional level of control in the PWM control scheme. This may be done by eliminating any switching states that result in common-mode voltages between the primary and secondary converters. Alternatively, the secondary bridge of the DID may be supplied by a floating dc capacitor with no power source, thus eliminating the common-mode circulating currents, see Fig. 1. The use of a floating bridge to supply the motor's secondary terminals reduces the size, weight, and cost of the system compared to a DID supplied by two dc sources.

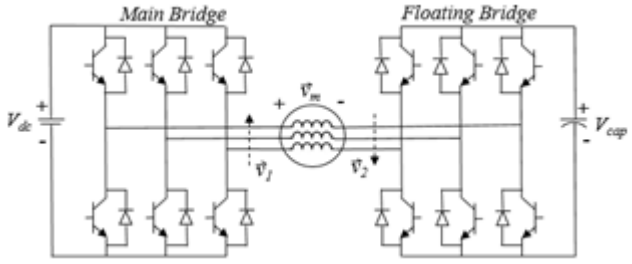

Fig.1. The dual inverter drive with a floating capacitor bridge

The DID topology with a floating bridge has been previously considered in literature for various applications. In the floating capacitor bridge is used to provide solely reactive voltage support to the motor and counteract supply voltage droop. Recently, the floating bridge has been utilized to produce three-level PWM motor voltages, while regulating the capacitor voltage at a ratio of 2:1 with the main dc supply voltage. In, this topology was implemented with an improved flux-oriented control scheme for high-speed applications. Furthermore, it has been shown that if left unregulated, the floating capacitor will naturally charge or discharge to a stable steady-state operating point dependant on the motor's current loading conditions.

The focus of the proposed control scheme is to maintain high motor efficiencies over a wide range of motor load settings and drive operating frequencies. The voltage boosting capability of the DID allows for improved motor performance in the speed range extension region. In addition, regulation of the floating capacitor voltage maintains the power factor of the main bridge close to unity and improves the system's stability during transient load changes. Similar to many common V/f motor drives, the proposed control scheme is not intended for applications that demand high-performance speed control, in which a flux-oriented control scheme is recommended.

II. PRINCIPLESOFOPERATION

The drive voltage phasors *v1* and *v2*, Fig. 1, represent the two components of the motor's per-phase fundamental voltage resulting from the main and floating bridges, respectively.

The phase difference between *v1* and*v2* is denoted by the angle *α*. *vm* is the per-phase voltage supplied to the stator's windings, and is the vector sum of *v1* and *v2*:

$$|\vec{v_1}| = \frac{m_1 V_{dc}}{2\sqrt{2}} \quad \ldots\ldots\ldots\ldots 1$$

$$|\vec{v_2}| = \frac{1.15 V_{cap}}{2\sqrt{2}} \quad \ldots\ldots\ldots 2$$

$$\vec{v_m} = \vec{v_1} + \vec{v_2} \quad \ldots\ldots\ldots\ldots 3$$

Where Vdc and Vcap are the supply dc voltage and the floating capacitor's dc voltage, respectively. The amplitude modulation index of the primary inverter, m1, is controllable, while the secondary inverter's amplitude modulation index is kept at its maximum value in order to minimize the voltage of the floating capacitor. The system has a natural tendency for the floating capacitor's voltage to reach a steady-state level, related to the motor's load conditions, when the motor's current phasor, im, is orthogonal to v2 with no net transfer of real power to the capacitor. Hence, the state of the capacitor is dependent on the instantaneous real power absorbed by the floating bridge:

$$P_2 = {}^3/_2 \, |\vec{v_2}| |\vec{i_m}| \cos\beta \quad \ldots\ldots\ldots 4$$

Where β is the angle formed between phasors im and v2. im may be projected onto the axis of v2 resulting in real and imaginary components, im,R and im,I. Assuming an ideal capacitor and power electronics, the real component of im will be zero when the system is at steady-state:

$$i_{m,R}^{SS} = 0 \quad \ldots\ldots\ldots 5$$

However, under non-ideal conditions there will be steady- state power consumed by the floating bridge due to the equivalent series resistance of the capacitor, as well as the switching and conduction losses in the power electronics. These steady-state power losses result in the steady-state angle β between im and v2 to be slightly less than 90°. For the remainder of the control scheme discussion these power losses will be neglected and β will be assumed to be 90° under steady-state operation.

The floating capacitor charging process is depicted in Fig. 2. Since β<90°, P2 will be positive, thus real power is absorbed by the floating bridge and the capacitor charges. Therefore, v2 will increase with the capacitor's voltage, moving vm and im anti-clockwise in the figure, until im,R relative to v2 reaches zero. Alternatively, the floating capacitor discharging process is shown in Fig. 3. Since β>90°, P2 will be negative, thus real power is injected by the floating bridge and the capacitor discharges. Therefore, v2 will decrease with the capacitor's voltage, moving vm clockwise in the figure until im,R reaches zero. Both the power factor angle of the motor and the magnitude of v1 directly influence the angle β, and thus influence the steady-state voltage level of the floating capacitor. While the motor's power factor angle is largely dependent on the motor's loading conditions, the magnitude of v1 is controlled by m1.

Therefore, m1 may be used as a control parameter to effectively regulate the voltage of the floating capacitor.

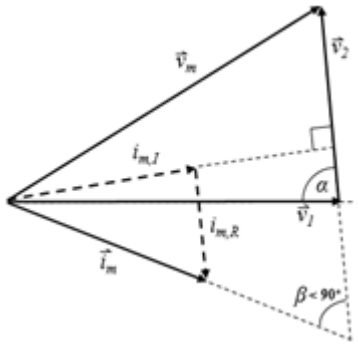

Fig.2. Operating point resulting in natural capacitor charging

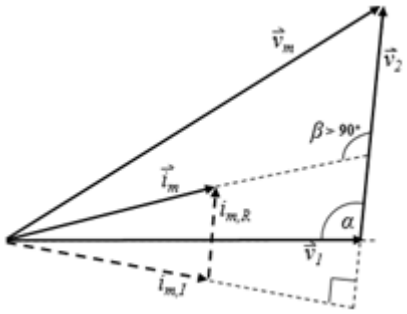

Fig.3.Operating point resulting in naturalcapacitordischarging

III. POWER FACTOR CONTROL FOR HIGH MOTOR EFFICIENCY

Maximizing the power conversion efficiency of the induction motor has many benefits for improving the operational lifetime of the machine and lowering the power drawn from the supply , especially useful when using a dc battery source. The maximum motor operating efficiency is associated with many parameters, but for this work is linked to the machine operating with a constant power factor by controlling the motor voltage, vm.

A. Induction Motor Control

Under the proposed control scheme, the motor's terminal voltage is controlled in order to maintain a constant power factor over the entire range of load settings and drive frequencies. This is achieved by modifying the angle α of the secondary bridge voltage injection. As a result of allowing the capacitor voltage to vary in the proposed manner, the DID can boost the motor voltage 41% higher than operating from a single bridge with full rated power. This can also result in a speed range extension of 41% without flux weakening. Using the induction motor's single phase equivalent circuit and parameters for the motor used in this work, examination revealed a motor power factor of 0.71 provided near optimal motor efficiency for drive frequencies between 10-60 Hz, see Fig. 4. Hence, the drive control described was developed to obtain a high motor power conversion efficiency at all drive frequencies and motor power levels using the relatively simple goal of maintaining the motor's power factor constant (0.71 for the chosen motor).

Signal feedback of the drive's two dc inverter voltages allow v1 and v2 to be known, and α may then be calculated in order to ensure the nominal motor power factor angle: θm=45°, see Fig. 5. If θm is 45° and β=90° is assumed under steady- state, then the angle γ between the reference motor voltage, v *, and v2 must also be 45° under steady-state conditions. Equation (6) may be written for the angle γ based upon the system's steady-state phasor diagram.

$$\cos(\gamma) = \cos(45°) = \frac{\left|\vec{v_m^*}\right|^2 + |\vec{v_2}|^2 - |\vec{v_1}|^2}{2\left|\vec{v_m^*}\right||\vec{v_2}|} \quad \ldots..6$$

v * may then be calculated using (6) and the quadratic formula, as defined in (7).

$$\left|\vec{v_m^*}\right| = \frac{2|\vec{v_2}|\cos(45°) + \sqrt{(2|\vec{v_2}|\cos(45°))^2 - 4(|\vec{v_2}|^2 - |\vec{v_1}|^2)}}{2} \quad \ldots7$$

Therefore, v^*_m may be updated based upon the calculated magnitudes of $v1$ and $v2$ in order to achieve the desired power factor for the motor. Once the reference motor voltage has been calculated, a value for the phase difference angle α_{cap} may be derived from the product of the per-unit drive frequency setting and the measured per-unit motor current. Under light loads and low drive frequencies, v^* for the chosen nominal power factor is greatly reduced. Therefore, $v2$ and V^* must be proportionally reduced in relation to both the motor's supply current and frequency, such that α remains in a stable operating range close to 90°. Values of α less than 60° and greater than 120° can lead to instability and voltage collapse in the capacitor's voltage. Thus, V^* is calculated using (10).

Obtained by using:

$$\alpha = \cos^{-1}\left[\frac{|\vec{v_1}|^2 + |\vec{v_2}|^2 - \left|\vec{v_m^*}\right|^2}{2|\vec{v_1}||\vec{v_2}|}\right] \quad \ldots.8$$

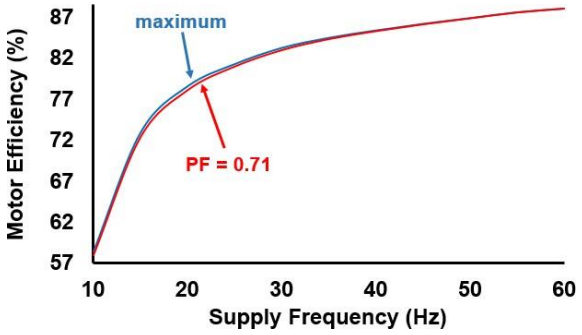

Fig. 4. Theoretical motor efficiency: maximum (blue), PF=0.71 (red)

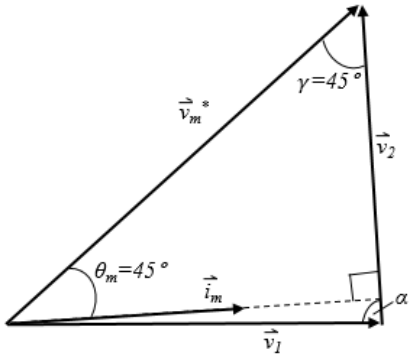

Fig. 5. Steady-state phasor diagram assuming θm=45°

In summary, the measured values of Vdc and Vcap are used to directly calculate the required fundamental phase difference between the main bridge and floating bridge in order to ensure the nominal motor power factor under steady-state operation.

B. Floating Capacitor Voltage Control

Since the magnitude of v1 directly influences the charging and discharging of the floating capacitor, the parameter m1 is used to control Vcap using a PI control block. The input to the PI compensator is the floating capacitor's voltage error, resulting in the following equation for m1 in the Laplace domain:

$$m_1 = \left(V_{cap}^{*} - V_{cap}\right)\left(\frac{K_p s + K_i}{s}\right) \quad (9)$$

Where K_p and K_i are the PI compensator's proportional and integral gains, respectively. The reference for V_{cap}, V_{cap} derived from the product of the per-unit drive frequency setting and the measured per-unit motor current. Under light loads and low drive frequencies, vm for the chosen nominal power factor must be is greatly reduced. Therefore, v2 and Vcap proportionally reduced in relation to both the motor's supply current and frequency, such that α remains in a stable operating range close to 90°. Values of α less than 60° and greater than 120° can lead to instability and voltage collapse in the capacitor's voltage. Thus, Vcap is calculated using (10).

$$V_{cap}^{*} = V_{cap}^{base} \times \left|\vec{i}_m^{pu}\right| \times f^{pu} \quad (10)$$

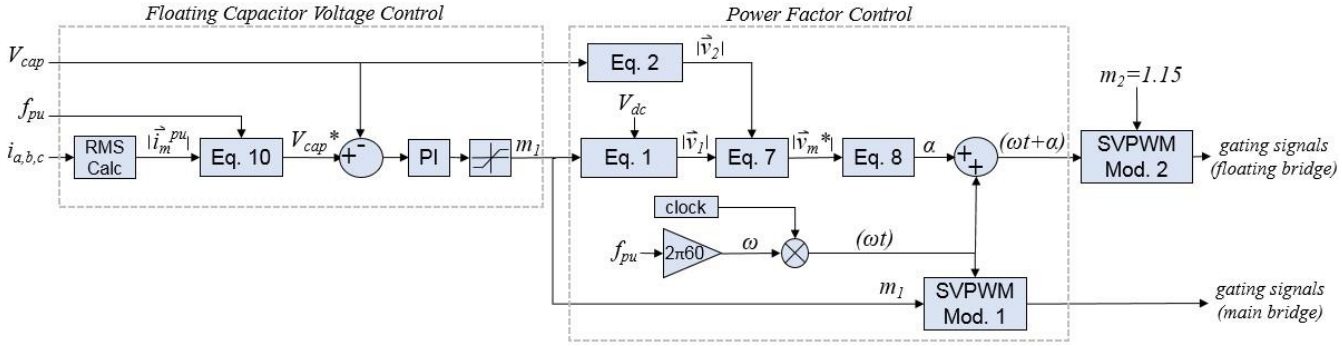

Fig. 6. Control block diagram

The base values for Vcap, im, and f are the dc supply voltage, rated full-load motor current, and rated motor frequency, respectively. In addition to keeping α within a stable operating range, the regulation of Vcap drastically improves the floating dc capacitor's voltage stability during transient load changes and maintains the power factor of the main bridge close to unity, thus decreasing the current drawn from the dc source. A block diagram of the entire control scheme is shown in Fig. 6.

IV. RESULTS

The DID topology under the proposed control strategy was simulated in both Simulink and Plecs in order to

verify the control of the floating capacitor voltage and confirm the predicted efficiency gains due to constant power factor operation. In order to quantify the benefits of the system, motor efficiencies are compared between the proposed control strategy and a conventional constant V/f control scheme operating with a single inverter drive. Experimental results were obtained using an open-ended winding 5 hp test motor. Results presented include measured experimental motor efficiencies as well as floating capacitor voltage behaviour during system start-up and motor load transients.

A. Simulation Results

Simulations of the proposed control strategy assumed: an input dc supply voltage of 300 V; a floating capacitor with a 4 mF capacitance; and that inverter gating signals were generated using the continuous space-vector PWM technique. The drive control was proven to be effective during steady-state operation by maintaining the nominal motor power factor of 0.71 for loads varying between zero and full load, and over a supply frequency range of 10-60 Hz.

To demonstrate the controller's transient response, the motor's load changed in 0.25 per-unit steps from 1-0.25 p.u. using a supply frequency of 60 Hz, see Fig. 7. At each load decrease vm is automatically reduced in order to maintain the motor's nominal power factor. As the load current decreases, so too does V * based upon (10). The PI compensator lowers m1 in order to track Vcap *, causing both v_1 and v_2 to be decreased. The control algorithm then updates the angle α based upon the current values of v1 and v2, thus supplying the appropriate terminal voltage to the motor. Once the transient in the motor's load current has finished, the system will reach a new steady-state operating point with the floating capacitor at a reduced voltage. This capacitor voltage control also maintains α in an acceptable range close to 90°, thus keeping the power factor of the main bridge close to unity. Without the action of the PI compensator in the feedback loop, the unregulated capacitor voltage is susceptible to large spikes at each step change in the load, Fig. 7. The motor speed can be observed to increase initially after each load decrease, before returning to the nominal speed corresponding to a motor power factor of
0.71.

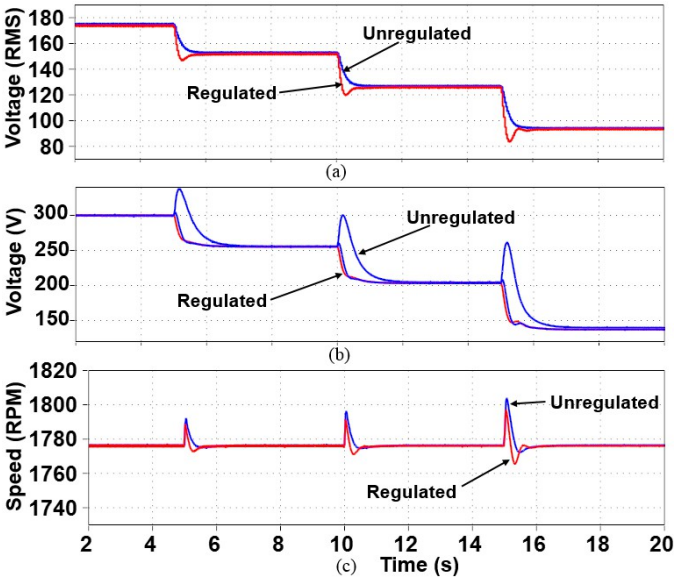

Fig. 7. Simulation results: (a) motor phase voltage; (b) capacitor voltage (blue) and reference (red); (c) motor speed

B. Experimental Results

The experimental testing conducted verifies the benefits of running the induction motor under constant power factor operation. A 4-pole, 230 V, 5 hp, 15 lb-ft, 60 Hz induction motor was operated at four drive frequencies: 15, 30, 45, and 60 Hz. The equivalent circuit parameters for the test motor are included in Table 1.

TABLE I. INDUCTION MOTOR PARAMETERS

P_{rated}	=	3.73	kW	R_s	=	0.3	Ω
$I_{s,rated}$	=	13	A	R_R	=	0.244	Ω
$V_{s,rated}$	=	230	V	X_s	=	0.697	Ω
f_s	=	60	Hz	X_R	=	0.544	Ω
p	=	2		X_M	=	19.671	Ω

Custom power electronics used Semikron (SKiM306GD12E4) IGBT modules with a 12 mF floating capacitor. A large capacitance was initially selected to increase the voltage stability of the floating capacitor. A 300 V Xantrex dc supply (XPR 300-20) was utilized to supply the main bridge. A MAGTROL dynamometer was used to load the motor, and the test system was controlled using the dSPACE DS1104 controller board, see Fig. 8. The motor's power conversion efficiency was obtained at the four drive frequencies tested, with the motor efficiency compared between using rated voltage constant V/f operation and using the proposed constant power factor controller, see Fig. 9. The 300 V dc source was not sufficient to supply the motor its rated voltage under 60 Hz operation from a single inverter

drive, therefore the motor was supplied from a voltage-boosting variac in this scenario. However, the voltage boosting capability of the DID enabled the use of the 300 V dc supply under 60 Hz operation. Firstly, the data shows good agreement between the theoretical and experimental results. Rated voltage V/f control results in classic efficiency variations with load: drooping slightly at high loads, and drooping rapidly under light loads. The power conversion efficiencies are highest under 60 Hz operation and decrease with each drive frequency setting down to 15 Hz. The efficiencies peak in the mid-torque region which coincide with the constant power factor operation curves. The constant power factor control resulted in elevated motor efficiencies, remaining fairly constant with decreasing load settings before beginning to droop at approximately 35% load. The largest gains in power conversion efficiency due to the proposed control scheme are under 15 Hz operation, in which constant power factor control showed efficiency increases of approximately 18% and 7% at 0.1 and 1 p.u. loads, respectively, when compared to V/f control.

The slip of an induction motor is closely related to its operating power factor, and thus the machine's slip also plays an important role in the overall power conversion efficiency of the motor. The constant power factor control scheme greatly reduced the variation in motor slip over the entire range of load settings when compared to V/f control, see Fig. 10. Under V/f control the variations in slip between 0.1 and 1 p.u. loads were 35 rpm and 49 rpm at 60 Hz and 15 Hz operation, respectively. The same slip variation value under constant power factor control was 10 rpm for each drive frequency setting tested. This is due to the constant power factor control algorithm automatically boosting the motor's voltage beyond the rated value under high load conditions, and decreasing the motor voltage under light loads.

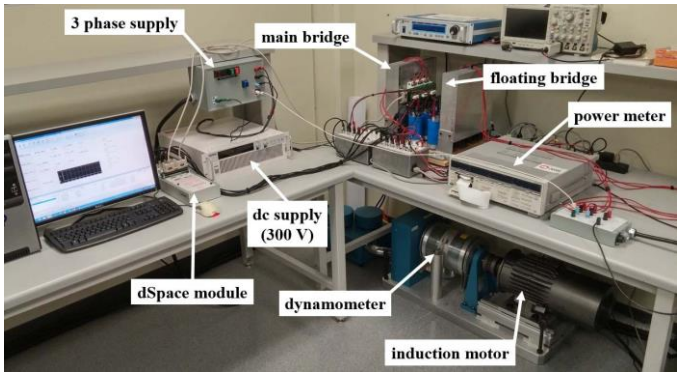

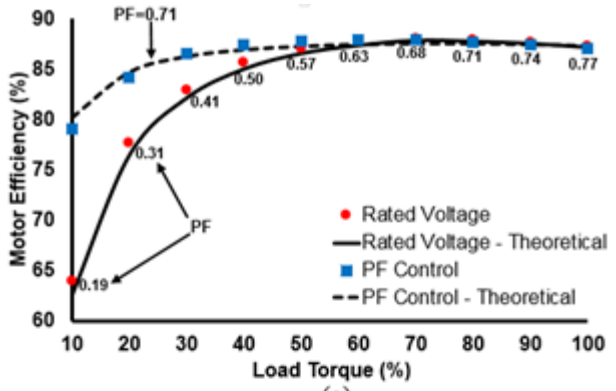

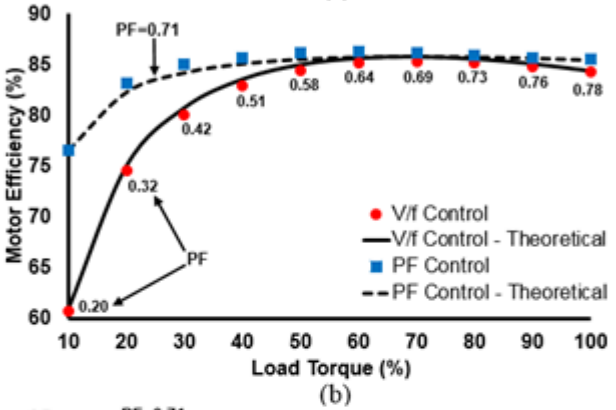

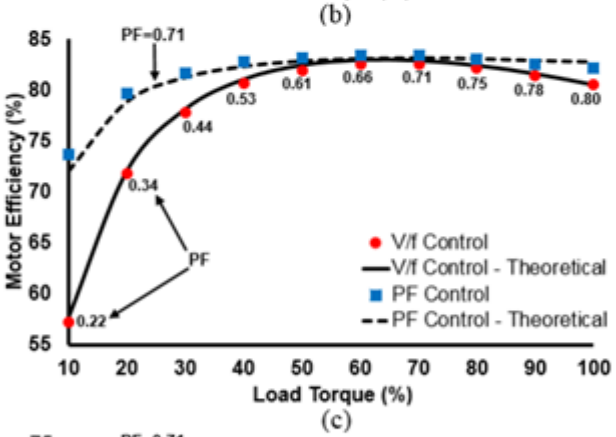

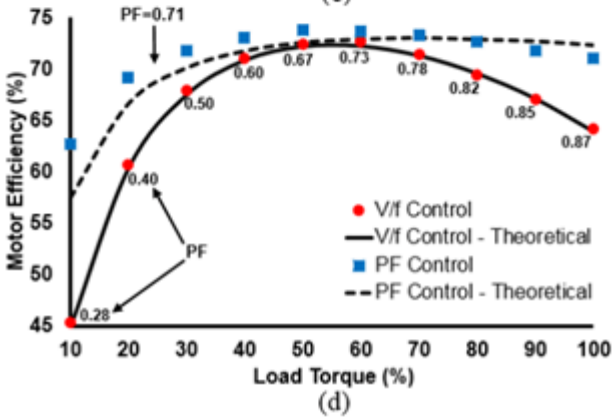

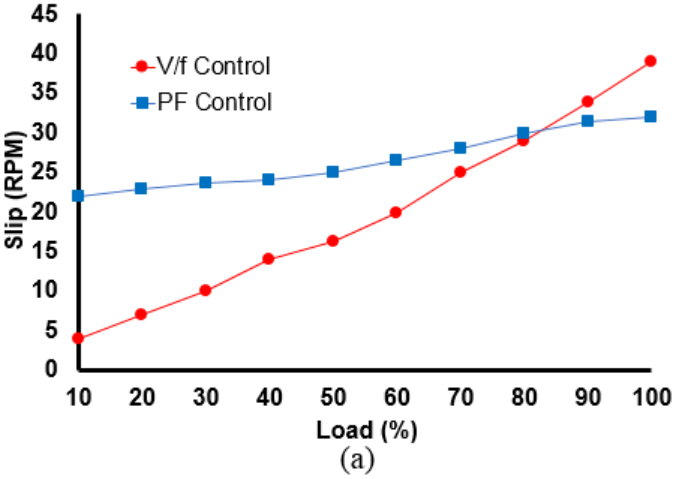

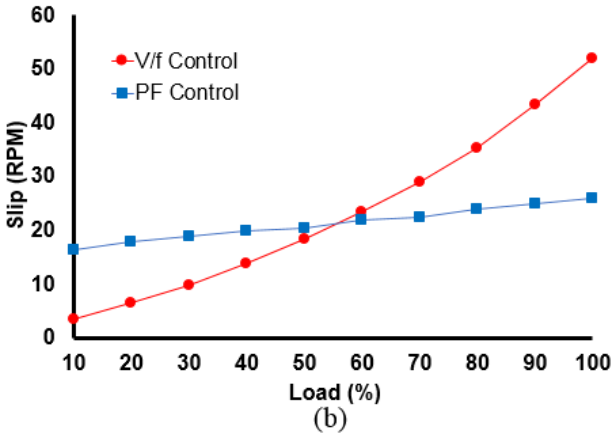

Fig. 10. Experimental results: motor slip under rated voltage and constant power factor control (a) 60 Hz (b) 15 Hz

To verify the controller's response to transient load changes, the motor's load was decreased in 0.25 per-unit steps from 1-0.25 p.u. using a supply frequency of 45 Hz, see Fig. 11. Once again, at each load decrease V * is reduced in a proportional manner to the motor's load current. Although vm is updated quickly based on real-time calculations, Vcap demonstrates a slow response due to the large dc-link capacitance utilized by the floating bridge. A smaller floating bridge capacitance would result in a quicker transient response by the system. One of the primary benefits of this method of capacitor control is that α is maintained close to 90° for all load settings. This keeps the power factor of the main bridge close to unity, which minimizes the dc current drawn by the main supply. Throughout all experimental testing of the proposed DID system the power factor of the main bridge remained between 0.984 leading and 0.983 lagging. An additional benefit of lowering Vcap under light loads is a reduction in the switching losses in the floating bridge. Device turn-on and turn-off losses are proportional to both the device current and dc-link voltage. This reduction of Vcap lowers the switching losses in the power electronics of the secondary converter, thus contributing to less power loss in the floating bridge, see Fig. 12. This power loss reduction leads to a more efficient motor drive system.

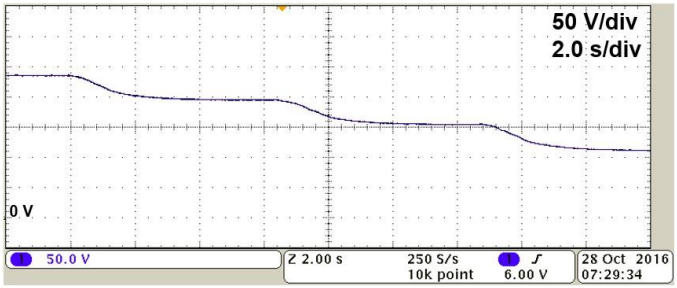

Fig. 11. Experimental results: floating capacitor voltage during transient load step changes (45 Hz operation)

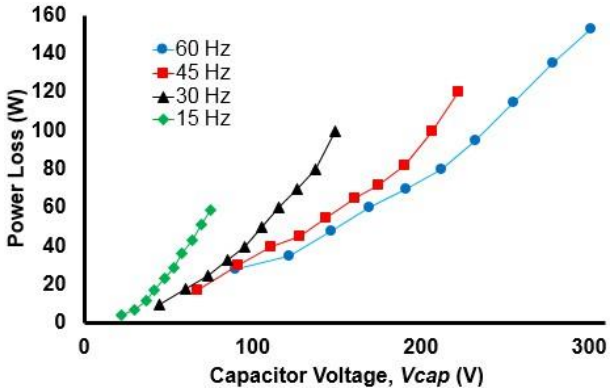

Fig. 12. Experimental results: power loss in the secondary bridge as a function of floating capacitor voltage

1) System Start-up

The system start-up procedure is comprised of four components. Firstly, the motor is started using a conventional soft-start method from solely the main converter. The three upper IGBT switches of the secondary converter remain closed during this process, in order to emulate a Y-connection at the motor's secondary terminals. Secondly, switching in the floating converter is enabled and the capacitor is pre-charged to an arbitrary value using the PI compensator of the control algorithm. Under 60 Hz operation the magnitude of Vcap upon pre-charging was set to 100 V, see Fig. 13. During this stage the phase difference angle α between the main and floating bridges is kept at 90°. Thirdly, the power factor control portion of the control scheme is enabled, thus allowing α to be updated appropriately. Lastly, the capacitor voltage reference signal, V *, is enabled based upon the drive's current frequency setting and motor current measurements.

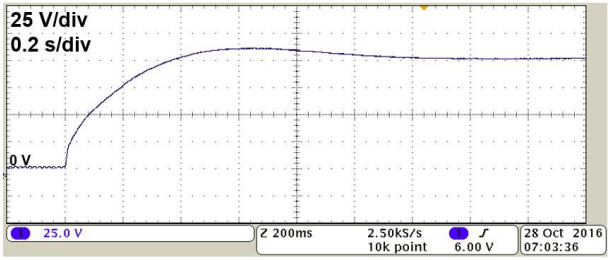

Fig. 13. Experimental results: floating capacitor voltage during start-up pre-charging

V. CONCLUSION

The proposed drive control is successfully demonstrated for an open-ended winding induction motor drive system using a dual inverter drive with a floating capacitor bridge. The controller can effectively regulate the motor's operating power factor over a wide range of loading conditions and drive frequencies. The controller includes an algorithm that: (a) changes the floating capacitor voltage as required under variable load and frequency operation, (b) stabilizes the floating capacitor voltage under step changes in the load. Constant motor power factor operation was tested using a 5 hp induction motor with variable frequency operation, demonstrating large efficiency gains over a wide load range when compared to a rated voltage constant V/f control scheme. The proposed method of floating capacitor voltage control further reduces the switching losses of the floating bridge under light loads, and maintains the power factor of the main converter near unity for all loading conditions and drive frequencies tested.

REFERENCES

[1] A. Edpuganti and A. Rathore, "New optimal pulsewidth modulation for single dc-link dual-inverter fed open-end stator winding induction motor drive," IEEE Trans. Power Electron., vol. 30, no. 8, pp. 4386-4393, Aug. 2015.

[2] J. Ewanchuk, J. Salmon, and C. Chapelsky, "A method for supply voltage boosting in an open-ended induction machine using a dual inverter system with a floating capacitor bridge," IEEE Trans. Power Electron., vol. 28, no. 3, pp. 1348-1357, Mar. 2013.

[3] J. Ewanchuk and J. Salmon, "A square-wave controller for high speed induction motor drive using a three phase floating bridge inverter," IEEE Energy Conv. Cong. and Expo. ECCE, pp. 2584-2591, 2010.

[4] R. Haque, A. Kowal, J. Ewanchuk, A. Knight, and J. Salmon, "PWM control of a dual inverter drive using an open-ended winding induction motor," IEEE Applied Power Electron. Conf. and Expo. APEC, pp. 150-156, 2013.

[5] S. Chowdhury, P. Wheeler, C. Patel, and C. Gerada, "A multilevel converter with a floating bridge for open-ended winding motor drive applications," IEEE Trans. Ind. Electron., vol. 63, no. 9, pp. 5366-5375, May 2016.

[6] S. Chowdhury, P. Wheeler, C. Gerada, and S. Arevalo, "A dual inverter for an open end winding induction motor drive without an isolation transformer," IEEE Applied Power Electron. Conf. and Expo. APEC, pp. 283-289, 2015.

[7] S. Chowdhury, P. Wheeler, C. Gerada, and C. Patel, "A dual two-level inverter with a single source for open end winding induction motor drive application," Euro. Conf. on Power Electron. And App. EPE-ECCE- Europe, pp. 1-9, 2015.

[8] H. Kubo, Y. Yamamoto, T. Kondo, K. Rajashekara, and B. Zhu, "Zero- sequence current suppession for open-end winding induction motor drive with resonant controller," IEEE Applied Power Electron. Conf. and Expo. APEC, pp. 2788-2793, 2016.

[9] V. Oleschuk et al., "Novel schemes of synchronous PWM for dual inverter-fed drives with cancellation of the zero sequence currents," IEEE Int. Symp. Power Electon., Electrical Drives Automation and Motion SPEEDAM, pp. 451-456, 2006.

[10] K. Ramachandrasekhar, S. Mohan, and S. Srinivas, "An improved PWM for a dual two-level inverter fed open-end winding induction motor drive," Int. Conf. on Electrical Machines ICEM, pp. 1-6, 2010.